Journal of Power Sources 198 (2012) 223–228

Contents lists available at SciVerse ScienceDirect

Journal of Power Sources

journal homepage: www.elsevier.com/locate/jpowsour

Preparation and electrochemical performance of TiO_2/C composite nanotubes as anode materials of lithium-ion batteries

Jingwei Zhang*, Xiangxia Yan, Jiwei Zhang, Wei Cai, Zhisheng Wu*, Zhijun Zhang

Key Laboratory of Ministry of Education for Special Functional Materials, Henan University, Kaifeng 475004, PR China

ARTICLE INFO

Article history:
Received 16 July 2011
Received in revised form 31 August 2011
Accepted 15 September 2011
Available online 21 September 2011

Keywords:
Titanium dioxide/carbon composite nanotubes
Lithium ion batteries
Anode material
Preparation
Electrochemical properties

ABSTRACT

A facile and scalable process is established to prepare titanium dioxide/carbon (TiO_2/C) composite nanotubes possessing a large specific surface area and an enhanced conductivity, with which H-titanate nanotubes are used as a precursor and glucose as a shape-stabilizing agent to retain the tubular morphology of the precursor during heat treatment. The effects of glucose dosage and calcination temperature on the microstructure and electrochemical properties of as-prepared TiO_2/C composite nanotubes are investigated. The results show that TiO_2/C composite nanotubes exhibit markedly improved electrochemical properties as compared with pristine TiO_2 sample. The incorporation of carbon helps to retain the tubular morphology of the precursor and improves the electrochemical properties of the target products. In general, the microstructure and electrochemical properties of as-prepared TiO_2/C composite nanotubes are closely dependent on the dosage of carbon and calcination temperature as well. The electrode made of TiO_2/C composite nanotubes calcinated at 400 °C, with a carbon content of 5%, possesses good high-rate capability (110 mAh g^{-1} at 20*C*) as well as excellent cycle life and capacity, showing promising application as an anode material for lithium-ion batteries.

1. Introduction

Titanium dioxide (TiO_2) possesses a much higher operating voltage (~1.7 V *vs.* Li^+ (1 M)/Li) than commonly used materials of carbon-based electrodes (~0.1 V *vs.* Li^+ (1 M)/Li), and it is chemically stable, inexpensive, nontoxic and abundant in nature [1]. Therefore, TiO_2 can be adopted as a promising anode material for lithium ion batteries to replace conventional carbon-based anode materials and increase the safety of the cells. However, TiO_2 has a low Li-ion diffusivity and electronic conductivity, which severely deteriorates its reversible capacity and high rate performance as an electrode material [2,3]. These drawbacks, fortunately, can be overcome by constructing nanostructured TiO_2 or by coating TiO_2 with highly electrically conductive materials. On one hand, by miniaturization of TiO_2 to nanometer size, the contact area between TiO_2 electrode and electrolyte is increased, the diffusion length for both Li ion and electron transport is shortened, and the durability against the strain of Li ion intercalation and extraction is increased. As a result, the electrochemical properties are significantly improved [4]. On the other hand, coating TiO_2 with materials of good electronic conductivity, carbon coating for example, can increase electronic conductivity and improve reversible capacity and high rate capability of TiO_2 [5–7]. Naturally, the electrochemical properties of TiO_2 should be more efficiently improved if nanoscale miniaturization is combined with coating by highly electrical conductive materials.

Bearing that perspective in mind, we are particularly interested in H-titanate nanotubes as a well-known candidate precursor for fabricating tubular TiO_2 nanostructure [8,9]. H-titanate nanotubes are thermally unstable and transformed to anatase TiO_2 during calcining above 400 °C, accompanied by collapse of tubular morphology [10]. This adds difficulty to fabrication of nanotubular TiO_2 from H-titanate nanotubes. Such a drawback, fortunately, could be overcome by introducing conductive materials during the fabrication of nanotubular TiO_2 from H-titanate nanotubes. Recently, Park et al. fabricated carbon coated TiO_2 nanotubes by combining hydrothermal reaction with post-calcination at 400 °C [11]. We found in our previous work that a relatively high reaction temperature (180 °C) was needed for glucose as a carbon source to be transformed into a kind of carbonaceous product (uncertain organic matter) under the above-mentioned hydrothermal conditions, and a carbon coating layer was formed *via* carbonization and graphitization of the carbonaceous organic matter during post-calcination [12]. We also found that the existence of the carbonaceous product helped to keep the tubular morphology of TiO_2 in annealing process [13]. H-titanate nanotubes are of particular interest as supporting materials for spontaneous monolayer dispersion of some organic matter onto its surface by way of the formation of

* Corresponding authors. Tel.: +86 378 3881358; fax: +86 378 3881358.
E-mail addresses: jwzhang@henu.edu.cn, jwzhang0378@yahoo.cn (J. Zhang).

0378-7753/$ – see front matter © 2011 Elsevier B.V. All rights reserved.
doi:10.1016/j.jpowsour.2011.09.039

ester-like linkage or chelation between H-titanate and organic matter *via* electrostatic attraction, hydrogen bonding, or chemical binding [14]. In the meantime, glucose ($C_6H_{12}O_6$) as a simple sugar contains one aldehyde group and five hydroxyl groups that can be linked to hydroxyls of H-titanate nanotubes by hydrogen bonding or chemical binding. Therefore, a quasi-solid-phase method was established in the present research to fabricate TiO_2/C composite nanotubes from using H-titanate nanotubes as the precursor and glucose as the coating carbon source. H-titanate nanotubes were prepared by a modified hydrothermal process under atmospheric pressure. As-prepared H-titanate nanotubes were then mixed with the aqueous solution of glucose and heated at 60 °C for more than 12 h until the mixed system was fully dried. Resultant dried mixture was finally calcinated at 400 °C to generate TiO_2/C composite nanotubes. Since the adding of carbon can improve the electronic conductivity and helps to retain the tubular morphology of nanostructured TiO_2 during calcination, and the route to synthesizing TiO_2/C composite nanotubes is cost-effective and easy to scale up, as-synthesized TiO_2/C composite nanotubes may possess improved reversible capacity and high rate capability and hence find promising application as a kind of anode materials for lithium ion batteries.

2. Experimental

2.1. Preparation of TiO_2/C composite nanotubes

TiO_2/C composite nanotubes were prepared *via* three steps. Firstly, H-titanate nanotubes were synthesized *via* a modified alkali hydrothermal treatment route [14]. Resultant precipitates were rinsed with distilled water to pH = 10 and kept in 0.1 M HCl solution for 10 h, followed by washing with distilled water to a pH value of about 7 and drying at 120 °C generating desired H-titanate nanotubes. Secondly, a proper amount of glucose was dissolved in distilled water and mixed with as-obtained H-titanate nanotubes (the amount of carbon (C:TiO_2 weight ratio) can be adjusted in a range of 0–10%). Resultant mixture was heated at 60 °C for more than 12 h to allow full drying. Finally, as-dried mixture was calcinated at 400 °C under Ar atmosphere, generating target TiO_2/C composite nanotubes denoted as TiO_2/C-2-400, TiO_2/C-5-400, TiO_2/C-7.5-400, and TiO_2/C-10-400, respectively; where numerical suffixes 2, 5, 7.5, and 10 refer to carbon to TiO_2 ratio, and numerical suffix 400 refers to calcination temperature. To investigate the effect of temperature on the structure and electrochemical performance of TiO_2/C composites, we also prepared TiO_2/C composites with a fixed carbon content of 5% using glucose as precursor at 300 °C and 500 °C, respectively. The corresponding composites were denoted as TiO_2/C-5-300 and TiO_2/C-5-500.

2.2. Characterization of TiO_2/C composites

X-ray diffraction (XRD) patterns of the products were collected using a Philips X'Pert Pro MPD X-ray diffraction system (Cu Kα radiation, λ = 0.15418 nm). Transmission electron microscopic (TEM) images were obtained using a JEOL JEM-2100 transmission electron microscope at an accelerating voltage of 200 kV. Cyclic voltammetric curves and electrochemical impedance spectra were obtained with a ZAHNER IM6ex electrochemical work station. Raman spectra were measured with RW-1000 laser Raman spectrometer. Moreover, a 3H-2000PS2 surface area tester (Beishide Instrument-ST Company Ltd., Beijing, China) was performed to measure the specific surface area (Brunauer–Emmett–Teller, abridged as BET) of the composites tester.

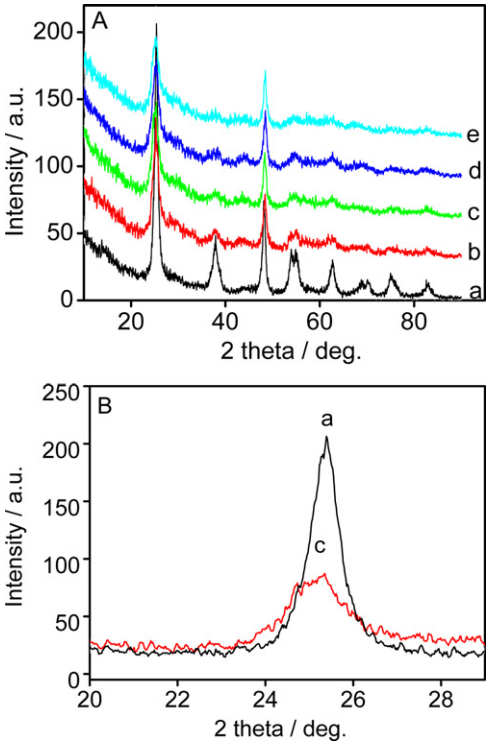

Fig. 1. (A) XRD patterns of (a) TiO_2 sample, (b) TiO_2/C-2-400, (c) TiO_2/C-5-400, (d) TiO_2/C-7.5-400, and (e) TiO_2/C-10-400; (B) partial enlarged XRD patterns of TiO_2 sample and TiO_2/C-5-400.

2.3. Preparation of electrodes made of TiO_2/C composites

The mixture of active materials (TiO_2 or TiO_2/C composite nanotubes), conductive agent (carbon black), and binder (polyvinylidene fluoride, abridged as PVDF) with a mass ratio (wt%) of 80:10:10 was dissolved in N-methyl-2-pyrrolidone and coated onto copper foils. As-coated copper foils were dried under vacuum at 120 °C for 12 h, and cut into plates with a size of about 15 mm and pressed, generating working electrodes. The working electrodes and Li metal counter electrode were assembled into cells by using Celgard 2400 as the separator and 1 M solution of $LiPF_6$ in ethylene carbonate and dimethyl carbonate (volume ratio 1:1) as the electrolyte. The cells were constructed in an Ar-filled glove box. The charge/discharge curves were measured using a LAND Cell tester (Wuhan, China) at a cutoff voltage of 3.0–1.0 V. Cyclic voltammetric curves were recorded in a voltage range of 1.0–2.2 V at a scan rate of 0.1 mV s^{-1}. The electrochemical impedance spectra were recorded by applying an alternating current of 5 mV in a frequency range from 0.01 Hz to 100 kHz.

3. Results and discussion

3.1. Characterization of TiO_2/C composites

Fig. 1 shows the XRD patterns of TiO_2/C composites. All the diffraction peaks can be indexed as anatase TiO_2, but with the increasing of carbon content, the diffraction peaks of the anatase TiO_2 become broader and their relative intensity decreases. This implies that adding carbon can influence the transformation of H-titanate to anatase TiO_2, and reduce the crystallinity of the final product. Besides, the peak shift of the (1 0 1) peak of TiO_2/C-5-400 anatase towards smaller angle direction as compared with that of pristine TiO_2 (see Fig. 1B) implies that the incorporation of carbon results in a larger (1 0 1) lattice spacing, which may benefit the kinetics of Li insertion/extraction.

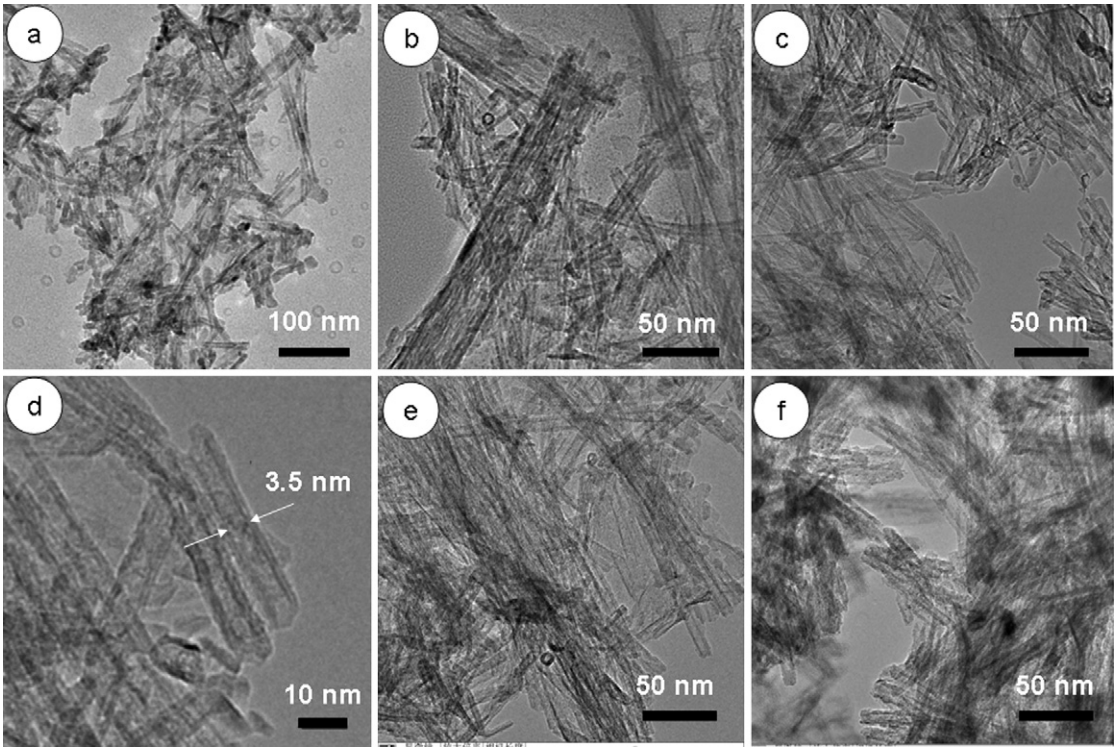

Fig. 2. TEM images of (a) TiO_2 sample, (b) TiO_2/C-2-400, (c) TiO_2/C-5-400, (d) partial enlarged image of (c), (e) TiO_2/C-7.5-400, and (f) TiO_2/C-10-400.

Fig. 2 shows the TEM images of TiO_2/C composite nanotubes with different carbon contents obtained after calcination at 400 °C. It can be seen that after heat treatment of H-titanate at 400 °C, resultant TiO_2 tends to aggregate and its tubular structure is almost completely destroyed (see Fig. 2a). However, TiO_2/C composite nanotubes retain the tubular structure after calcination under the same condition (see Fig. 2b–f). Besides, TiO_2/C composite nanotubes calcinated at 400 °C have a much larger specific surface area than pure TiO_2 sample (see Table 1), well corresponding to the tubular morphology. This means that TiO_2/C composite nanotubes possess easier accessibility to electrolyte, which is beneficial to improving the reversible capacity and high rate capability of the composite as a kind of lithium ion battery anode materials. Fig. 2d, partial enlarged image of Fig. 2c, indicates that as-prepared TiO_2/C composite nanotubes have an inner diameter of about 3.5 nm, which is consistent with BJH pore size distribution result (approximately 3.3 nm, see Fig. 3). Interestingly, although thermally unstable H-titanate nanotubes experience collapse of tubular morphology and are transformed into anatase TiO_2 during calcination above 400 °C [10], glucose helps to retain the nanotubular morphology during calcinations. The reason may lie in that glucose molecule contains one aldehyde group and five hydroxyl groups which can be linked to the hydroxyls on H-titanate nanotubes by hydrogen bonding or other chemical bonding. As a result, TiO_2/C composites with well retained tubular structure are obtained after calcination.

Table 1
The BET of TiO_2 and TiO_2/C composite nanotubes obtained after calcination at 400 °C.

Sample	BET specific surface area ($m^2\ g^{-1}$)
Pristine TiO_2	168.3
TiO_2/C-2-400 (2%C)	254.1
TiO_2/C-5-400 (5%C)	253.5
TiO_2/C-7.5-400 (7.5%C)	245.7
TiO_2/C-10-400 (10%C)	243.2

3.2. Electrochemical properties of TiO_2/C composites

Fig. 4 shows the cyclic performance of TiO_2/C composite nanotubes calcined at 400 °C at rates of 0.5–20.0*C*. It can be seen that TiO_2/C composite nanotubes exhibit better rate performance than TiO_2 sample. Namely, the specific capacity of TiO_2 sample fades rapidly with increasing rate, and it significantly decreases from 174 mAh g^{-1} at 0.5*C* to 54 mAh g^{-1} at 10*C*. TiO_2/C-5-400 possess stable discharge capacities of 240 mAh g^{-1}, 215 mAh g^{-1}, 192 mAh g^{-1}, 176 mAh g^{-1}, 160 mAh g^{-1}, 138 mAh g^{-1} and 110 mAh g^{-1} at a discharge rate of 0.5*C*, 1*C*, 2*C*, 3*C*, 5*C*, 10*C*, and 20*C*, respectively, which are mostly higher than 150 mAh g^{-1} at 1*C* reported by Pol et al. [15]. Here, what role does the glucose play in preparation of titanium dioxide/carbon composite nanotubes and in improvement of the electrochemical performance of the sample? Firstly, the carbon, derived from thermal decomposition of glucose, can improve the conductivity of the composite nanotubes [16]. Secondly, the glucose acts as a

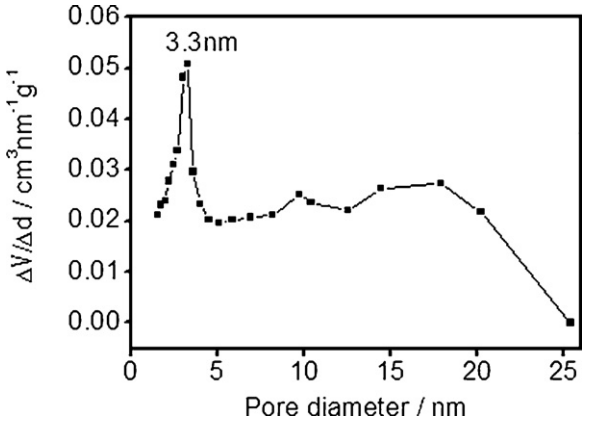

Fig. 3. BJH pore size distribution curves of TiO_2/C-5-400.

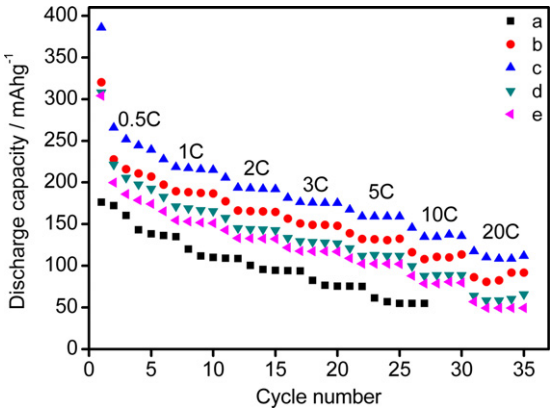

Fig. 4. Rate performance of (a) TiO_2 sample, (b) TiO_2/C-2-400, (c) TiO_2/C-5-400, (d) TiO_2/C-7.5-400, and (e) TiO_2/C-10-400.

shape-stabilizing agent to retain the tubular morphology of H-titanate during heat treatment (see Fig. 2), which resulted in increased specific surface area as well as better reversible capacity and high rate capability. Two effects mentioned above lead to an improved electrochemical performance of sample, the latter, differing from what has been reported elsewhere [7,17], may be worth special emphasis. However, glucose can also play an undesirable effect, namely, reducing the crystallinity of the product (seen from XRD results in Fig. 1), which will lower the conductivity and structural stability of composite nanotubes. Thereby, the electrochemical performance of products, such as reversible capacity and cycle stability will be degenerated. So, there will be an appropriate amount of carbon needed in TiO_2/C composite nanotubes for best electrochemical performance. The experimental results show that the suitable carbon content is about 5%. Besides, from the TEM images in Fig. 2, it can be seen that TiO_2/C-5-400 seems to have best dispersibility and smoothest surface. All of reasons mentioned above make TiO_2/C-5-400 showing the best electrochemical performance among all the TiO_2/C composite nanotubes samples.

In order to compare the cyclic stability of the electrodes made of TiO_2 and TiO_2/C composite nanotubes obtained at 400 °C, we evaluated their cyclic performance at a discharge rate of 10*C*. As shown in Fig. 5, all the tested samples have stable cycle life and almost unchanged capabilities after 100 cycles. Fig. 6a shows the initial five charge/discharge curves of TiO_2 electrode at 0.5*C*. There is a plateau of discharge at about 1.7 V and a plateau of charge at about 2.0 V. The first discharge and charge capacity are 235.3 mAh g^{-1} and 180.4 mAh g^{-1}, respectively, corresponding to first coulombic efficiency of 76.7%. The coulombic efficiency

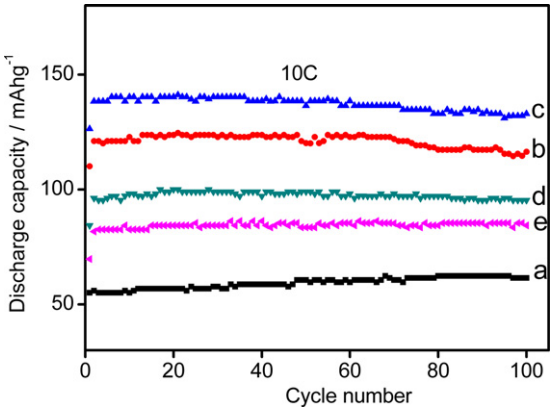

Fig. 5. Cycle performance of (a) TiO_2 sample, (b) TiO_2/C-2-400, (c) TiO_2/C-5-400, (d) TiO_2/C-7.5-400, and (e) TiO_2/C-10-400.

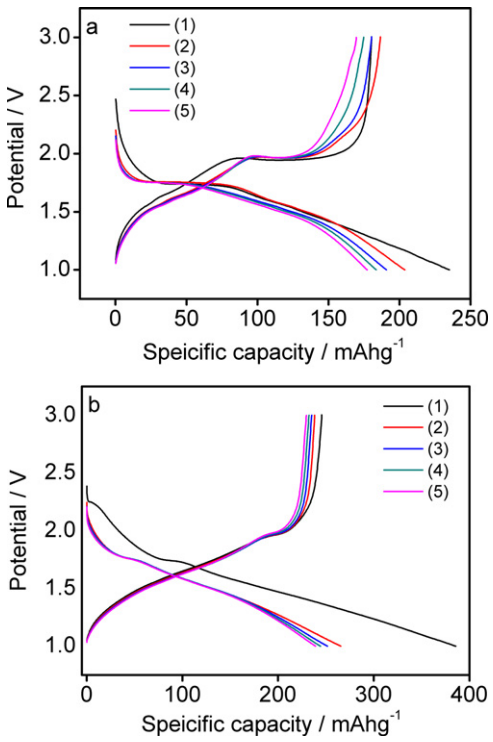

Fig. 6. The initial five charge/discharge curves of (a) TiO_2 sample and (b) TiO_2/C-5-400.

reaches 91.4% at the second cycle of charge/discharge, and it rises to 95.7% at the fifth charge/discharge cycle. Fig. 6b shows the initial five charge/discharge curves of TiO_2/C-5-400 at 0.5*C*. Its first discharge reaches 385.8 mAh g^{-1}, exceeding relevant theoretical capacity (335 mAh g^{-1}). However, a big irreversible capacity loss of 140 mAh g^{-1} emerges from first discharge cycle (385.8 mAh g^{-1}) to first charge cycle (245.7 mAh g^{-1}), corresponding to a coulombic efficiency of 63.8%. Low conductivity of TiO_2 inevitably results in an apparent polarization effect during charge/discharge process, especially at a high rate. More importantly, the side reactions involving water molecules chemically or physically absorbed on the internal and/or external surface of TiO_2 nanotubes may also cause the decrease of coulombic efficiency in the initial charge/discharge stage [1]. The bigger irreversible capacity loss of TiO_2/C-5-400 as compared with TiO_2 may be attributed to their bigger specific surface area (see Table 1). However, it can be seen that the first coulombic efficiency of 63.8% of TiO_2/C composite nanotubes (TiO_2/C-5-400) quickly increase to 96% after fifth cycle at a rate of 0.5*C*. As the charge/discharge cycle proceeds, the coulombic

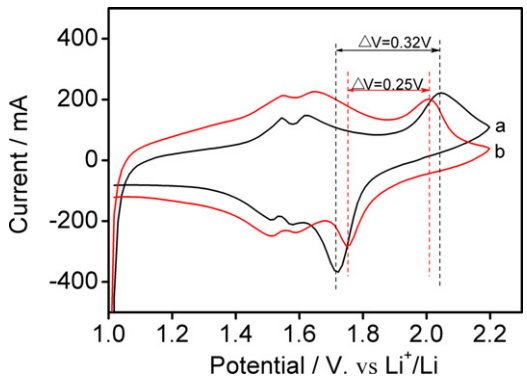

Fig. 7. The cycle voltammograms of (a) TiO_2 sample and (b) TiO_2/C-5-400.

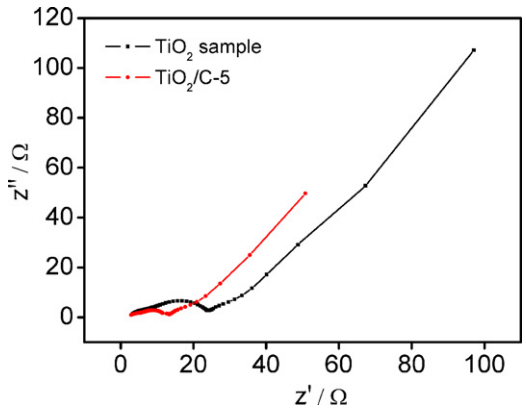

Fig. 8. The AC impedance spectra of TiO_2 sample and TiO_2/C-5-400.

efficiency increases further to 99–101% after 10th cycle. Here, the measured value exceeds 100%, probably due to the measurement error (shown in supporting information, Figs. S1 and S2).

The discharge process of the TiO_2 and TiO_2/C nanotubes electrode follows a three-step mechanism. The first step is a topotactic insertion into Li-poor compound Li_xTiO_2, where x value is dependent on particle size. The second step involves phase transition from Li_xTiO_2 (anatase, $I41/amd$) to Li_yTiO_2 (orthorhombic distortion, $Imma$), where, the longer voltage plateau of TiO_2 sample, comparing with the TiO_2/C composite nanotubes, attributes to the better crystallinity as evidenced by XRD peaks. The third step involves another topotactic insertion into Li-rich compound Li_yTiO_2 [18].

Fig. 7 displays the cycle voltammograms (CVs) of TiO_2 sample and TiO_2/C-5-400 sample at a scan rate of 0.1 mV s^{-1}. Usually, a single cathodic peak corresponding to lithium insertion and a single anodic peak corresponding to lithium extraction are observed in anatase TiO_2 [19]. For TiO_2 sample, the cathodic/anodic peaks, corresponding to lithium insertion/extraction in the crystal lattice of anatase TiO_2, are centered at 1.72 V and 2.04 V (with peak separation being 0.32 V). And the cathodic/anodic peaks of TiO_2/C-5-400 sample are centered at 1.76 V and 2.01 V (with peak separation being 0.25 V). The peak separation between anodic and cathodic peaks can reflect the polarization degree of the electrode. And obviously, sample TiO_2/C-5-400 has a lower potential difference than sample TiO_2, showing weaker polarization of the electrode owing to the incorporation of conductive carbon.

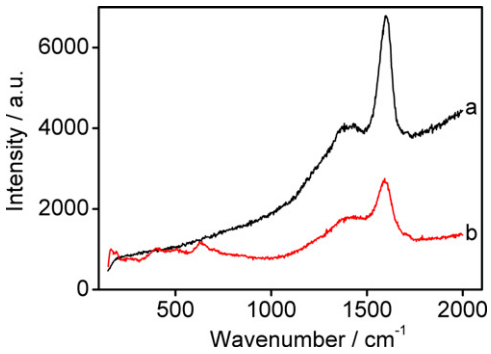

Fig. 9. Raman spectra of (a) pure carbon prepared by calcinating glucose at 400 °C and (b) TiO_2/C-5-400.

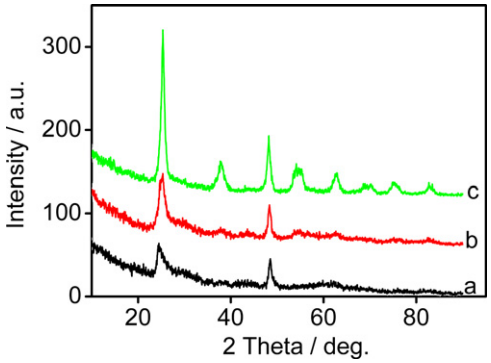

Fig. 10. XRD patterns of (a) TiO_2/C-5-300, (b) TiO_2/C-5-400, and (c) TiO_2/C-5-500.

The AC impedance plots of TiO_2 sample and TiO_2/C-5-400 sample prepared at 400 °C are presented in Fig. 8. It can be observed that they all comprise a semicircle in middle-frequency range and a sloping line in low frequency range. It is well known that the middle-frequency semicircle relates to the charge transfer through the electrode/electrolyte interface, and the sloping line at low frequency reflects the solid-state diffusion of Li-ions in bulk materials [20]. As it can be seen in Fig. 8, the semicircle diameter of TiO_2/C-5-400 electrode is smaller than that of the TiO_2 electrode, which indicates that TiO_2/C-5-400 sample has a smaller charge-transfer resistance than TiO_2 sample.

To investigate the structure of carbon in TiO_2/C nanotubes, we conducted Raman analysis. Fig. 9 shows the Raman spectra of pure carbon prepared by calcinating glucose at 400 °C and

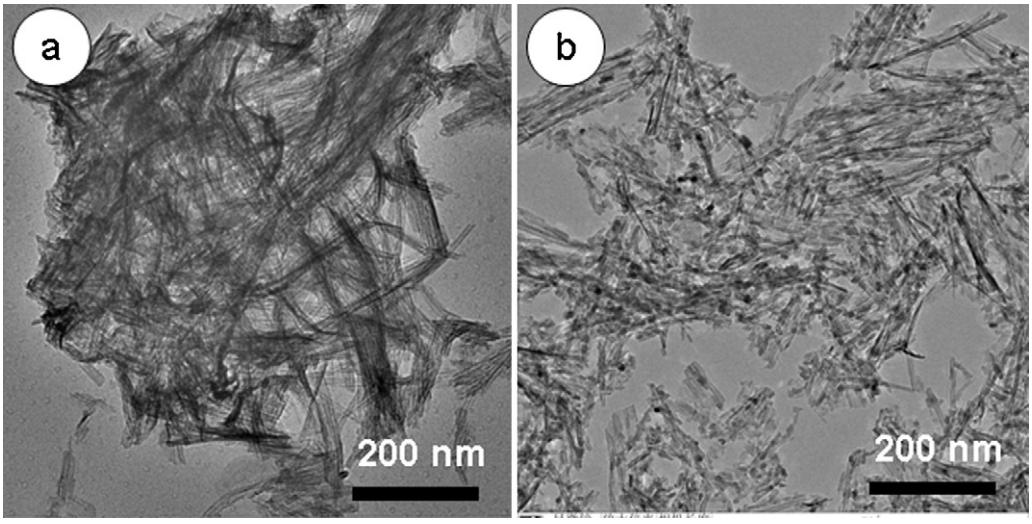

Fig. 11. TEM images of (a) TiO_2/C-5-300 and (b) TiO_2/C-5-500.

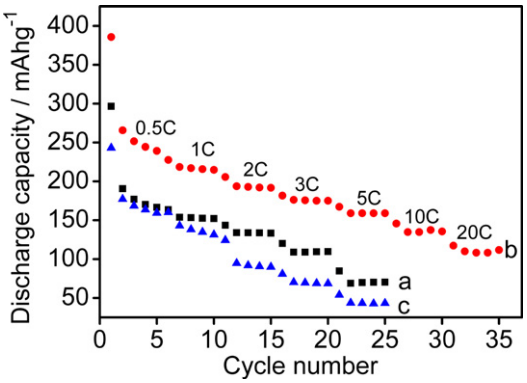

Fig. 12. Rate performance of (a) TiO_2/C-5-300, (b) TiO_2/C-5-400, and (c) TiO_2/C-5-500.

of TiO_2/C-5-400. The absorption bands at 408 cm^{-1}, 506 cm^{-1}, and 627 cm^{-1} correspond to anatase TiO_2 [21]. The intense broad band around 1440 cm^{-1} and 1590 cm^{-1} can be ascribed to the characteristic Raman spectra of carbon. Namely, the band around 1590 cm^{-1}, the G band, is attributed to graphitized carbon; and that at about 1440 cm^{-1}, the D band, corresponds to disordered carbon [22,23]. The graphitized carbon contains sp^2 hybrid bonding, which is positively correlated with the electronic conductivity of carbon, and the disordered carbon mainly corresponds to sp^3 hybrid bonding. Carbons obtained by calcinating glucose and TiO_2/C-5-400 at 400 °C have integrated sp^2/sp^3 intensity ratios of 0.60 and 0.68, respectively, which shows that TiO_2 /C-5-400 has a lower degree of graphitization than carbon derived from glucose. This is related to the interaction between TiO_2 nanotubes and glucose, and such an interaction helps to prevent the destruction of morphology of TiO_2 nanotubes during heat treatment.

Since the electrode made of TiO_2/C-5-400 composite possessed the best electrochemical performance, the effect of temperature on the structure and electrochemical performance of TiO_2/C composite nanotubes was investigated while the glucose content was fixed at 5%. Fig. 10 shows the XRD patterns of resultant TiO_2/C composite nanotubes (C:TiO_2 = 5:95) obtained after calcination at 300 °C, 400 °C, and 500 °C. It is seen that the crystallinity of anatase TiO_2 rises with elevating temperature. In the meantime, the composite obtained after calcination at 400 °C retains tubular structure (see in Fig. 2c and d), but after calcination at 500 °C the tubular structure of the composite is destroyed to form nanoparticles (see Fig. 11b). Fig. 12 shows the rate performance of the electrodes made of composites TiO_2/C-5-300, TiO_2/C-5-400, and TiO_2/C-5-500. TiO_2/C-5-400 possesses the best rate capacity, because it well retains tubular structure and has improved conductivity and crystallinity.

4. Conclusions

TiO_2/C composite nanotubes were prepared by calcinating the mixture of H-titanate nanotubes as the precursor and glucose as the carbon source. The effects of dosage of glucose and calcination temperature on the microstructure and electrochemical properties of TiO_2/C composite nanotubes were investigated. It was found that adding carbon not only improved the electronic conductivity but also helped to retain the tubular structure of the precursor during heating treatment. As a result, as-prepared TiO_2/C composite nanotubes have large surface area and good electronic conductivity. The electrode made of TiO_2/C-5-400 possesses increased capacity, stable cycling behavior, and good rate performance, showing promising application as an anode material for lithium-ion batteries.

Acknowledgments

We acknowledge financial support from National Natural Science Foundation of China (Grant Nos. 50902045/E0213 and 20971037/B0111), Foundation of Scientific Committee of Henan Province of China (Grant No. 082102270040) and Foundation of Educational Committee of Henan Province of China (Grant Nos. 2008A150004 and 2010GGJS-040).

Appendix A. Supplementary data

Supplementary data associated with this article can be found, in the online version, at doi:10.1016/j.jpowsour.2011.09.039.

References

[1] G.F. Ortiz, I. Hanzu, T. Djenizian, P. Lavela, J.L. Tirado, P. Knauth, Chem. Mater. 21 (2009) 63.
[2] S. Bach, J.P. Pereira-Ramosa, P. Willmanc, Electrochim. Acta 55 (2010) 4952.
[3] D.V. Bavykin, J.M. Friedrich, F.C. Walsh, Adv. Mater. 18 (2006) 2807.
[4] Y.F. Wang, M.Y. Wu, W.F. Zhang, Electrochim. Acta 53 (2008) 7863.
[5] S.J. Park, H. Kim, Y.J. Kim, H. Lee, Electrochim. Acta 56 (2011) 5355.
[6] L.J. Fua, L.C. Yanga, Y. Shia, B. Wanga, Y.P. Wu, Microporous Mesoporous Mater. 117 (2009) 515.
[7] J.W. Xu, Y.F. Wang, Z.H. Li, W.F. Zhang, J. Power Sources 175 (2008) 903.
[8] J.W. Zhang, X.Y. Guo, Z.S. Jin, S.L. Zhang, J.F. Zhou, Z.J. Zhang, Chin. Chem. Lett. 14 (2003) 419.
[9] J.J. Yang, Z.S. Jin, X.D. Wang, W. Li, J.W. Zhang, S.L. Zhang, X.Y. Guo, Z.J. Zhang, Dalton Trans. 20 (2003) 3898.
[10] M. Zhang, Z.S. Jin, J.W. Zhang, X.Y. Guo, J.J. Yang, W. Li, X.D. Wang, Z.J. Zhang, J. Mol. Catal. A 217 (2004) 203.
[11] S.J. Parka, Y.J. Kimb, H. Lee, J. Power Sources 196 (2011) 5133.
[12] Q.J. Li, J.W. Zhang, B.B. Liu, M. Li, S.D. Yu, L. Wang, Z.P. Li, D. Liu, Y.Y. Hou, Y.G. Zou, B. Zu, T. Cui, G.T. Zou, Cryst. Growth Des. 8 (2008) 1812.
[13] W. Wang, J.W. Zhang, H.Z. Huang, Z.S. Wu, Z.J. Zhang, Appl. Surf. Sci. 253 (2007) 5393.
[14] X.P. Gao, Y. Lan, H.Y. Zhu, J.W. Liu, Y.P. Ge, F. Wu, D.Y. Song, Electrochem. Solid State Lett. 8 (2005) A26.
[15] V.G. Pol, S.H. Kang, J.M. Calderon-Moreno, C.S. Johnson, M.M. Thackeray, J. Power Sources 195 (2010) 5039.
[16] S.K. Das, M. Patel, A.J. Bhattacharyya, ACS Appl. Mater. Interfaces 2 (2010) 2091.
[17] S.K. Das, A.J. Bhattacharyya, J. Phys. Chem. C 113 (2009) 17367.
[18] L. Aldon, P. Kubiak, A. Picard, J.C. Jumas, J. Olivier-Fourcade, Chem. Mater. 18 (2006) 1401.
[19] X. Gao, H. Zhu, G. Pan, S. Ye, Y. Lan, F. Wu, D. Song, J. Phys. Chem. B 108 (2004) 2868.
[20] J. Xie, X.B. Zhao, G.S. Cao, M.J. Zhao, Electrochim. Acta 50 (2004) 2725.
[21] L. Qian, Z.L. Du, S.Y. Yang, Z.S. Jin, J. Mol. Struct. 749 (2005) 103.
[22] M.A. Montes-Morán, R.J. Young, Carbon 40 (2002) 845.
[23] P. Delhaesa, M. Couzib, M. Trinquecostea, J. Dentzerc, H. Hamidouc, C. Vix-Guterlc, Carbon 44 (2006) 3005.